A theoretical treatment of the magnetic resonance properties of Sc and Ru

1993 J. Phys.: Condens. Matter 5 1707

(http://iopscience.iop.org/0953-8984/5/11/011)

J. Phys.: Condens. Matter 5 (1993) 1707–1720. Printed in the UK

A theoretical treatment of the magnetic resonance properties of Sc and Ru

W Götz and H Winter

Kernforschungszentrum Karlsruhe, Institut für Nukleare Festkörperphysik, PO Box 3640, W-7500 Karlsruhe, Federal Republic of Germany

Received 21 October 1992, in final form 15 December 1992

Abstract. We evaluate the low-temperature susceptibilities, the Knight shifts, and the spin–lattice relaxation times of the hexagonal d transition metals Sc and Ru and give a detailed account of the individual contributions expressed through magnetic correlation functions. The results are in reasonable agreement with tabulated experimental data for Sc and very recent measurements for Ru.

1. Introduction

Nuclear magnetic resonance properties of metals have received continuous experimental and theoretical attention during the past few decades since they shed light on the electronic structures, yielding information not immediately deducible from the bandstructures. Both the coupling between nuclear spin and the orbital motion and the spins of the electrons are probed. In addition, the different responses of the core electrons and the valence electrons and the interactions between them lead to distinct contributions to the Knight shifts (K) and the spin–lattice relaxation times (T_1) whose significance can be judged term-by-term by considering data for the susceptibility, χ_0, in addition. This opens up the possibility of investigating such delicate questions as the quality of the various exchange–correlation potentials used in spin density functional approach (SDFA) as a function of the electronic density (Götz and Winter 1991) and—most important in the case of the ceramic high-T_c materials—to test the validity of the SDFA for the system in question (Götz and Winter 1992a).

Theoretically, the situation is rather comforting, since, based on the pioneering work of Jaccarino (1967) and Narath (1967) where the basic formulations can be found, all the contributions to these quantities may be expressed in terms of magnetic correlation functions and the way the functions are calculated preserves the individuality of the given system expressed by the characteristics of its electronic structure.

Experimentally the investigations have gone so far as to measure K under pressure (Bertani *et al* 1990). However, for a number of interesting systems, experimental data are not yet available. In the case of the hexagonal d transition metal Ru data for K have only recently been obtained (Burgstaller *et al* 1992). We found it therefore worthwhile to apply our SDFA–RPA approach to correlation functions to calculate K, T_1 and χ_0 for Ru and for comparison also for the 3d transition metal Sc.

0953-8984/93/111707+14$07.50

The present paper is organized as follows. In section 2 we summarize the formalism, collecting the relevant relations and emphasizing the necessity to consider the dependence of the correlation functions on all their variables. In section 3 we present our KKR bandstructure calculations and display and discuss our results in section 4. We close with a summary in section 5.

2. Formalism

To describe the properties in question quantitatively we need, apart from the one-particle Green's function, the spin density $\chi^s_{\alpha\beta}$ and the momentum density $\chi^{\mathrm{mom}}_{\alpha\beta}$ correlation functions. Here, α, β are cartesian components. Each component, $\chi_{\alpha\beta}(\boldsymbol{r},\boldsymbol{r}';\omega)$, depends on two space coordinates $\boldsymbol{r}$, $\boldsymbol{r}'$ and a frequency variable, ω. In the local representation a coordinate $\boldsymbol{r}$ located within the Wigner–Seitz (WS) cell of site κ in the unit cell j at position $\boldsymbol{R}_j$ may be defined by the following relation: $\boldsymbol{r} = \boldsymbol{\rho} + \boldsymbol{\tau}^{\kappa} + \boldsymbol{R}_j = (\boldsymbol{\rho}, \kappa, j)$. Here, $\boldsymbol{\rho}$ is the coordinate relative to site κ. If the position $\boldsymbol{r}$ is in the central unit cell ($\boldsymbol{R}_j = 0$) we simply write: $\boldsymbol{r} = (\boldsymbol{\rho}, \kappa)$. In the case of a crystalline solid it is appropriate to work with the lattice Fourier transforms, $\chi_{\boldsymbol{q}}$, of χ, defined through the following equation

$$\chi_{\boldsymbol{q}}(\boldsymbol{\rho}\kappa, \boldsymbol{\rho}'\kappa';\omega) = \chi^{\kappa\kappa'}_{\boldsymbol{q}}(\boldsymbol{\rho}, \boldsymbol{\rho}';\omega) = \sum_j \mathrm{e}^{\mathrm{i}\boldsymbol{q}\boldsymbol{R}_j} \chi(\boldsymbol{\rho}\kappa, \boldsymbol{\rho}'\kappa' j;\omega). \tag{2.1}$$

Once $\chi_{\boldsymbol{q}}$ is known the diagonal part of the real-space double Fourier transform, $\chi(\boldsymbol{q},\boldsymbol{q};\omega)$, of $\chi(\boldsymbol{r},\boldsymbol{r}';\omega)$ may be obtained via the following relation

$$\begin{aligned}\chi(\boldsymbol{q},\boldsymbol{q};\omega) &= \sum_{\kappa,\kappa'} \chi^{\kappa\kappa'}(\boldsymbol{q},\boldsymbol{q};\omega) \\ &= \sum_{\kappa,\kappa'} \int \mathrm{d}\boldsymbol{\rho}\, \mathrm{e}^{-\mathrm{i}\boldsymbol{q}\cdot(\boldsymbol{\rho}+\boldsymbol{\tau}^{\kappa})} \int \mathrm{d}\boldsymbol{\rho}'\, \mathrm{e}^{\mathrm{i}\boldsymbol{q}\cdot(\boldsymbol{\rho}'+\boldsymbol{\tau}'^{\kappa'})} \chi^{\kappa\kappa'}_{\boldsymbol{q}}(\boldsymbol{\rho},\boldsymbol{\rho}';\omega).\end{aligned} \tag{2.2}$$

The quantity $\chi(\boldsymbol{q},\boldsymbol{q};\omega)$ is usually referred to as the wavevector-dependent correlation function. We evaluate both χ^{mom} and χ^s within the SDFA–RPA, namely express χ^{mom} and the non-interacting part χ^{Ps} of χ^s in terms of the bandstructure one-particle Green's function, $g_{\boldsymbol{q}}(\boldsymbol{\rho}\kappa, \boldsymbol{\rho}'\kappa';\epsilon)$, whereas the potential, K_{xc}, giving rise to the enhancement effects of χ^s is gained from the SDFA. The contributions of the core electrons have been treated separately from the valence electrons and are labelled 'core' in the following formulae. The details of this method and various applications have been described in previous papers (e.g. Stenzel and Winter, 1985, 1986, Winter *et al* 1992). To enable discussion of our results, we therefore restrict ourselves to collecting the relevant expressions.

Neglecting spin–orbit coupling the static homogeneous susceptibility, χ_0, is determined through the following relations (Götz and Winter 1992b)

$$\chi_{0\alpha\beta} = \chi_{\mathrm{spin}\alpha\beta} + \chi_{\mathrm{orb}\alpha\beta} \tag{2.3}$$

with

$$\chi_{\mathrm{spin}\alpha\beta} = \lim_{\boldsymbol{q}\to 0} \sum_{\kappa,\kappa'} \chi^{s\kappa\kappa'}_{\alpha\alpha}(\boldsymbol{q},\boldsymbol{q};\omega)\delta_{\alpha\beta} \tag{2.4}$$

and

$$\begin{aligned}\chi_{\mathrm{orb}\alpha\beta} &= \chi^{\mathrm{val}}_{\mathrm{orb}\alpha\beta} + \chi^{\mathrm{dia,core}}_{\mathrm{orb}}\delta_{\alpha\beta} \\ \chi^{\mathrm{val}}_{\mathrm{orb}\alpha\beta} &= \sum_{\substack{\gamma\delta \\ \nu\mu}} \epsilon_{\alpha\gamma\delta}\epsilon_{\mu\nu\beta} \lim_{\boldsymbol{q}\to 0} \frac{q_\gamma}{q^2}(\chi^{\mathrm{mom}}_{\delta\mu}(\boldsymbol{q},\boldsymbol{q};0) - \chi^{\mathrm{mom}}_{\delta\mu}(0,0;0))\frac{q_\nu}{q^2}.\end{aligned} \tag{2.5}$$

Due to $\chi^{\mathrm{val}}_{\mathrm{orb}}$ the value of the susceptibility depends on the direction of the external magnetic field and we did calculations for both $\boldsymbol{H}$ parallel ($\beta = 3$) and $\boldsymbol{H}$ perpendicular ($\beta = 1$ or 2) to the c axis of the HCP structure.

The expression for the Knight shift K is based on the non-relativistic hyperfine Hamiltonian, $\mathcal{H}_{\mathrm{hf}}$, (Bloembergen and Rowland, 1953) and gives rise to a decomposition into the spin contact ($K_{\mathrm{s,c}}$), the spin dipolar ($K_{\mathrm{s,dip}}$), the paramagnetic orbital ($K_{\mathrm{orb,para}}$) and the diamagnetic orbital part ($K_{\mathrm{orb,dia}}$). They depend both on the position κ of the nuclear spin and on the direction β of the magnetic field and are defined through the following relations

$$K^{(\kappa,\beta)}_{\mathrm{s,c}} = \lim_{q\to 0}\sum_{\kappa'}\frac{8\pi}{3}\int \mathrm{d}\rho'\,\chi^{s\kappa\kappa'}_{q\beta\beta}(0,\rho';0)$$

$$K^{(\kappa,\beta)}_{\mathrm{s,dip}} = -\lim_{q\to 0}\sum_{\alpha\kappa'}\int \mathrm{d}\rho\,\mathrm{d}\rho'\left(\frac{\delta_{\alpha\beta}}{\rho^3}-\frac{3\rho_\alpha\rho_\beta}{\rho^5}\right)\chi^{s\kappa\kappa'}_{q\alpha\beta}(\rho,\rho';0)$$

$$K^{(\kappa,\beta)}_{\mathrm{orb,para}} = -\lim_{q\to 0}\sum_{\substack{\alpha\mu\nu\\ \gamma\delta\kappa'}}\epsilon_{\alpha\gamma\delta}\epsilon_{\mu\nu\beta}\int \mathrm{d}\rho\,\mathrm{d}\rho'\frac{\rho_\gamma}{\rho^3}\chi^{\mathrm{mom}\kappa\kappa'}_{q\delta\mu}(\rho,\rho';0)\frac{q_\nu}{q^2}\mathrm{e}^{\mathrm{i}q\cdot\rho'}$$

$$K^{(\kappa,\beta)}_{\mathrm{orb,dia}} = -\frac{2}{3}\int \mathrm{d}\rho\, n^{\kappa}_{\mathrm{core}}(\rho)\frac{\rho^2}{\rho^3}. \tag{2.6}$$

Here, $n^{\kappa}_{\mathrm{core}}$ is the charge density of the core electrons of atom κ. The core polarization term, $K^{(\kappa,\beta)}_{\mathrm{cp}}$, has to be added to these contributions. All the formulae on the RHS of (2.6) are given in atomic units (au), and to get the percentage Knight shifts the numbers have to be multiplied with a factor of 2.6626×10^{-5}.

To derive the expression for the spin lattice relaxation time, T_1, we write, following Moriya (1963), $1/T_1$ in terms of the fluctuations of the hyperfine Hamiltonian $\mathcal{H}_{\mathrm{hf}}$ in the limit of small frequencies, ω_0, ($\hbar\omega_0 \ll k_{\mathrm{B}}T$). This relation reads

$$\frac{1}{T_1} = \frac{\gamma_{\mathrm{N}}^2}{2}\int \mathrm{d}t\,\tfrac{1}{2}\cos\omega_0 t\langle \mathcal{H}^{+}_{\mathrm{hf}}(t)\mathcal{H}^{-}_{\mathrm{hf}}(0)+\mathcal{H}^{-}_{\mathrm{hf}}(0)\mathcal{H}^{+}_{\mathrm{hf}}(t)\rangle. \tag{2.7}$$

γ_{N} is the nuclear gyro-magnetic ratio and $\mathcal{H}^{\pm}_{\mathrm{hf}} = \mathcal{H}_{\mathrm{hf}x} \pm \mathrm{i}\mathcal{H}_{\mathrm{hf}y}$. Neglecting spin–orbit coupling effects and making use of the fluctuation dissipation theorem we obtain the following expression for $1/T_1$ in terms of the correlation functions:

$$\begin{aligned}\frac{1}{T_1} = \frac{4\pi k_{\mathrm{B}}T}{\hbar}(\hbar\gamma_{\mathrm{N}}\mu_{\mathrm{B}})^2\sum_{\alpha,\gamma}(1-\delta_{\alpha\beta})\int\frac{\mathrm{d}q}{\Omega_{\mathrm{BZ}}}\int\mathrm{d}\rho\int\mathrm{d}\rho'\,(F^{\mathrm{s}}_{\alpha\gamma}(\rho)\\ \times \mathrm{Im}(\mathrm{e}^{\mathrm{i}q\cdot\rho}\frac{1}{\omega_0}\chi^{s\kappa\kappa}_{q\gamma\gamma}(\rho,\rho';\omega_0)\mathrm{e}^{-\mathrm{i}q\cdot\rho'})F^{\mathrm{s}}_{\alpha\gamma}(\rho')+F^{\mathrm{o}}_{\alpha\gamma}(\rho)\\ \times \mathrm{Im}(\mathrm{e}^{\mathrm{i}q\cdot\rho}\frac{1}{\omega_0}\chi^{\mathrm{mom}\kappa\kappa}_{q\gamma\gamma}(\rho,\rho';\omega_0)\mathrm{e}^{-\mathrm{i}q\cdot\rho'})F^{\mathrm{o}}_{\alpha\gamma}(\rho'))\end{aligned} \tag{2.8}$$

where β is the direction of the external magnetic field and the space-dependent coupling tensors for the spin part are given by

$$F^{\mathrm{s}}_{\alpha\gamma}(\rho) = F^{\mathrm{s,c}}_{\alpha\gamma}+F^{\mathrm{s,dip}}_{\alpha\gamma} = \frac{8\pi}{3}\delta_{\alpha\gamma}\delta(\rho)-\left(\frac{\delta_{\alpha\gamma}}{\rho^3}-\frac{3\rho_\alpha\rho_\gamma}{\rho^5}\right) \tag{2.9}$$

and those for the orbital part by

$$F^{\mathrm{o}}_{\alpha\gamma}(\rho) = -\sum_{\mu}\epsilon_{\gamma\alpha\mu}\frac{\rho_\mu}{\rho^3}. \tag{2.10}$$

F^s is the sum of the contact term $F^{s,c}$ and the dipolar contribution $F^{s,dip}$. The quadrupolar terms, finite in the case of HCP structure, will be treated separately.

In contrast to χ_0 and K, evaluation of $1/T_1$ requires knowledge of the dynamical correlation functions in the low-frequency limit over the whole Brillouin zone (BZ). However, if one neglects enhancement effects, that is to say, if one replaces χ^s with the non-interacting susceptibility, χ^{Ps}, in (2.8), $1/T_1$ can be rigorously expressed through symmetry-adapted partial DOS at ϵ_F and space integrals over products of radial wavefunctions, determining the so-called hyperfine fields. A large number of terms resulting from such an approximate treatment have been derived for the HCP structure by Asada and Terakura (1982) and we take over their definitions when presenting our calculated data.

Addressing enhancement effects one should keep in mind that it is hard to establish a general relation between a wavevector- and site-dependent Stoner factor defined by

$$S(q) = \chi^{s\kappa\kappa}(q,q;0)/\chi^{Ps\kappa\kappa}(q,q;0)$$

on the one hand and the ratio

$$\operatorname{Im}\chi_q^{s\kappa\kappa}(\rho,\rho';\omega_0)/\operatorname{Im}\chi_q^{Ps\kappa\kappa}(\rho,\rho';\omega_0)$$

relevant for equation (2.8) on the other. To treat this problem quantitatively we use the following representation of χ_q^s, derived by Stenzel and Winter (1985):

$$\chi_q^{s\kappa\kappa'}(\rho,\rho';\omega_0) = \sum_{\substack{l_1l_2\nu_1\nu_2\\L_1M_1}} \sum_{\substack{l_3l_4\nu_3\nu_4\\L_2M_2}} Y_{L_1M_1}(\hat\rho)R_{l_1\nu_1}(\rho)R_{l_2\nu_2}(\rho)Y_{L_2M_2}(\hat\rho')R_{l_3\nu_3}(\rho')$$

$$\times R_{l_4\nu_4}(\rho')\hat\chi_q^{s\kappa\kappa'}(L_1M_1l_1l_2\nu_1\nu_2|L_2M_2l_3l_4\nu_3\nu_4;\omega_0). \tag{2.11}$$

Here, the Y_{LM} are real spherical harmonics and $R_{l\nu}(\rho)$ is the νth ρ-dependent energy expansion coefficient of the radial part of the single-site wavefunction, $R_l(\rho,\epsilon)$ around $\epsilon = \epsilon_F$. The elements of $\hat\chi^s$ comprise these labels ν_i and the angular momentum numbers. The ratio of $\hat\chi^s$ to $\hat\chi^{Ps}$ turns out to depend sensitively on the matrix element in question and also to be strongly q-dependent. In this connection one should note that in the case of d transition metals contributions with L_i, $M_i = 0$ and $l_i = 2$ are especially important for $\chi^s(q,q;\omega)$, whereas the terms with L_i, M_i, $l_i = 0$ determine the spin contact part of $1/T_1$.

The formulae displayed in this section refer to the non-relativistic limit. If for a particular substance we use a scalar relativistic bandstructure, the radial integrals occurring in these expressions should be modified according to the rules as derived by Blügel *et al* (1987) and Ebert and Akai (1992).

3. The bandstructures

We performed scalar relativistic KKR bandstructure calculations on a prism mesh of 2100 k-points in the irreducible wedge of the Brillouin zone (IWBZ) for both substances in the HCP structure. For exchange and correlation, the potentials of von Barth and Hedin (1972) have been used.

The total and the angular momentum decomposed DOS for Sc are shown in figure 1 and the 20 lowest bands along the main symmetry directions are displayed in figure 2. The peak structure between about 0.3 Ryd and 0.8 Ryd is dominated by d states with a non-negligible admixture of s states at the lower end and p states,

especially in the vicinity of the Fermi energy, ϵ_F. ϵ_F falls into a local mimimum within the fine structure of the lowest pronounced d peak, causing the relatively high DOS value of 30.18 states/(Ryd atom). The corresponding numbers for the s, p, d and f partial DOS are 0.497, 7.64, 21.38, and 0.666, respectively. Within the structure above 0.9 Ryd, the DOS values are moderate and the proportions of the p and f states become comparable to those of the d states. To test convergence in the angular momentum expansion we did also runs with $l_{max} = 4$ and conclude that g scattering starts to become non-negligible only above 2 Ryd.

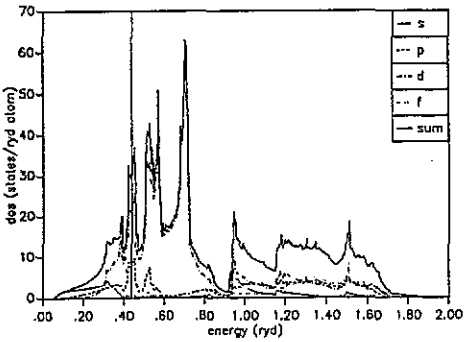

Figure 1. The s, p, d, and f partial DOS and the total DOS (sum) for Sc calculated for the 20 lowest valence bands. The vertical line at $\epsilon = 0.437$ Ryd designates the Fermi energy.

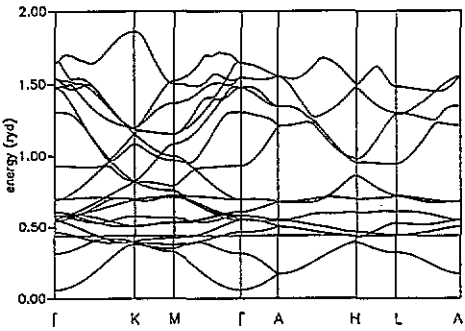

Figure 2. The lowest 20 valence bands of Sc along some symmetry directions within the IWBZ. The Fermi surface ($\epsilon_F = 0.437$ Ryd) is built up by the bands 3 and 4.

In the energy regime where comparison is possible our results are in general agreement with the work of Das (1976), MacDonald and Vosko (1979), and Matsumoto *et al* (1991). The latter authors show that a fully relativistic treatment yields slightly smaller numbers for the DOS at ϵ_F.

We show the corresponding data for Ru in figure 3 and figure 4. Similarly to Sc the DOS curve of Ru consists of a low-energy structure of mainly d states followed by a low-DOS and a moderate-DOS regime above 1.5 Ryd with appreciable s, p, d, and f partial DOS admixture. g states become important above $\simeq 3$ Ryd. The details, however, are markedly different. In the case of Ru ϵ_F lies in an extended mimimum between bonding and anti-bonding d states leading to the relatively low DOS value of 11.78 states/(Ryd atom) and the numbers 0.141, 0.783, 10.51, 0.347 for the s, p, d, and f partial DOS, respectively. The agreement of our results with the bandstructure work of Jepsen *et al* (1975) is reasonable.

Comparing our bandstructure data for Sc and Ru we expect marked differences in those quantities mainly determined by Fermi surface properties, e.g. the spin-dependent contributions to the susceptibility and the Knight shift. However, the orbital quantities can also be assumed to show a significant variance because of the pronounced differences in the DOS features in a finite energy range around ϵ_F.

4. Results and discussion

4.1. The static homogeneous susceptibilities

The values for the different contributions defined in (2.4) and (2.5) for scandium are

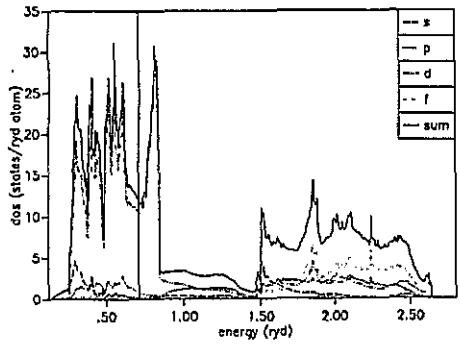

Figure 3. The s, p, d, and f partial DOS and the total DOS (sum) for Ru calculated for the 20 lowest valence bands. The vertical line at $\epsilon = 0.7135$ Ryd designates the Fermi energy.

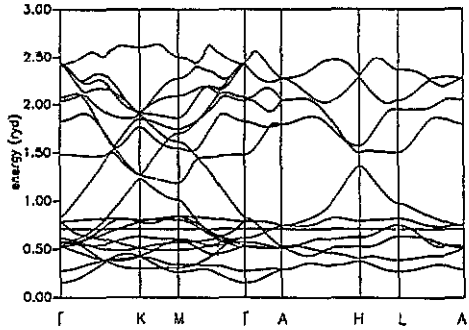

Figure 4. The lowest 20 valence bands of Ru along some symmetry directions within the IWBZ. The Fermi surface ($\epsilon_F = 0.7135$ Ryd) is built up by the bands 7 to 10.

displayed in table 1. Both χ_{orb} and χ_{spin} are significant and χ_{orb} shows appreciable anisotropy, whereas the core contribution, $\chi_{orb}^{dia,core}$, is only a small correction. We investigated the sensitivity of χ_{spin} on a number of exchange–correlation potentials, V_{xc} frequently used in applications of the SDFA. The results are also contained in table 1 together with the abbreviations of the authors of these potentials and the corresponding references. This appreciable dependence of S on V_{xc} can be understood by noting that enhancement effects are determined by the radial integrals of K_{xc}, the derivative of V_{xc} with respect to the magnetization density, between the product of four radial wavefunctions and for Sc the most important one reads

$$\langle K_{xc}\rangle = \int_0^{R_{WS}} \rho^2 \, d\rho K_{xc}(\rho) R_2^4(\rho, \epsilon_F). \tag{4.1}$$

The integrand of the RHS of (4.1) assumes its largest values near the WS sphere boundary ($\rho = R_{WS}$) where K_{xc} reaches its maximum and the magnitude of $R_2(\rho, \epsilon_F)$ is still fairly large. The electronic density there corresponds to $r_s = 2.42$ and, in line with our previous treatment of the alkali metals Li and Na (Götz and Winter 1991), the data for the different K_{xc} considered show a large scatter in this density range. Our $\langle\chi_0\rangle$ based on K_{xc}^{VWN} is near the experimental numbers 388×10^{-6} emu mol^{-1} and 393×10^{-6} emu mol^{-1}, obtained by Spedding and Croat (1973) and Stierman *et al* (1983). Concerning these uncertainties our results for χ_{spin} are reasonably close to the theoretical numbers 293.4, 281.25 and 270×10^{-6} emu mol^{-1} of Das (1976), MacDonald and Vosko (1979) and Matsumoto *et al* (1991) respectively, who used the variational principle (Vosko and Perdew 1975) to get the Stoner enhancement. Our value for the directionally averaged χ_{orb}^{val}, $\langle\chi_{orb}^{val}\rangle = 101.39 \times 10^{-6}$ emu mol^{-1} is slightly smaller than the result of Das (1976) for the van Vleck term, $\langle\chi_{orb}^{vV}\rangle = 127.8 \times 10^{-6}$ emu mol^{-1}. However, according to Benkowitsch and Winter (1982) $\langle\chi_{orb}^{val}\rangle$ also contains the Landau contribution and the diamagnetic contribution of the valence electrons.

Our data for Ru are shown in table 2. Except for $\chi_{orb}^{dia,core}$ all contributions to χ_0 are much smaller than in the case of Sc. For χ_{spin} this is an immediate consequence of the much lower DOS values $n(\epsilon_F)$ at ϵ_F leading to a reduction of the non-interacting susceptibility χ^{Ps}—and even more efficiently—of S to 1.34. For this substance χ_{spin}

Table 1. The static homogeneous susceptibility of Sc in units of 10^{-6} emu mol^{-1}. The averaged value of the total susceptibility is defined as $\langle\chi_0\rangle = \frac{1}{3}(\chi_{0\parallel} + 2\chi_{0\perp})$. The Stoner enhancement factors $S = \chi_{spin}/\chi^{P}_{spin}$ have been evaluated using our result $\chi^{P}_{spin} = 71.68 \times 10^{-6}$ emu mol^{-1}.

	Orbital susceptibility				Spin susceptibility		
	χ^{val}_{orb}	$\chi^{dia,core}_{orb}$	χ_{orb}	K_{xc} used	χ_{spin}	S	$\langle\chi_0\rangle$
$H\|\|c$	123.88	−10.47	113.41	VBH[a]	230.61	3.22	332.77
$H\perp c$	90.15	−10.47	79.68	PZ[b]	217.06	3.03	319.23
				JMW[c]	323.51	4.51	425.68
				GL[d]	298.49	4.16	400.66
				R[e]	230.61	3.22	332.77
				VWN[f]	262.29	3.66	364.46

[a] von Barth and Hedin (1972).
[b] Perdew and Zunger (1981).
[c] Janak *et al* (1975).
[d] Gunnarsson and Lundqvist (1976).
[e] Rajagopal (1980).
[f] Vosko *et al* (1980).

hardly depends on the choice of K_{xc} and this is due to both the magnitude of $n(\epsilon_F)$ and to the higher electronic density of Ru ($r_s = 1.72$ at R_{WS}). In table 2 we therefore quote only the two results for χ_{spin} showing the largest differences. The connection between χ^{val}_{orb} and the DOS features on the other hand is less obvious. Making use of the Kramers–Kronig relation btween the real and the imaginary part of χ_{orb} we found that an energy range around ϵ_F of about 0.4 Ryd in the case of Ru and 0.35 Ryd for Sc provides the main contributions to this quantity. The significant differences of the electronic structures of Sc and Ru in this regime are clearly represented by the DOS curves (figures 1 and 2). Sc especially profits from the fact that ϵ_F is surrounded by a high d DOS structure.

Table 2. The static homogeneous susceptibility for Ru in units of 10^{-6} emu mol^{-1}. Our value of χ^{P}_{spin} is 27.99×10^{-6} emu mol^{-1}.

	Orbital susceptibility				Spin susceptibility		
	χ^{val}_{orb}	$\chi^{dia,core}_{orb}$	χ_{orb}	K_{xc} used	χ_{spin}	S	$\langle\chi_0\rangle$
$H\|\|c$	20.68	−11.41	9.27	PZ	37.60	1.34	47.18
$H\perp c$	21.15	−11.41	9.74	JMW	38.48	1.37	48.06

The experiments of Kojima *et al* (1961), Isaacs and Lam (1970), and Guthrie and Bourland (1931) performed at room temperature, also yield small numbers for $\langle\chi_0\rangle$, namely 34, 41, and 43×10^{-6} emu mol^{-1}, respectively, lying somewhat below our result.

4.2. The Knight shifts

In our calculations we augmented the formulae of section 2 with the radial integrals applying to the scalar relativistic case (Blügel *et al* 1987). The numbers of table 3, where we list K together with its individual contributions for Sc, show the tendency of cancellation between the spin parts due to the appreciable and negative value of the

core polarization term, K_{cp}. K_{cp} is composed of the contributions −0.025, −0.1614, and −0.033%, from the 1s, 2s and 3s core shells of Sc leading to the corresponding core polarization hyperfine fields -6.42×10^3, -4.15×10^4, and -8.46×10^3 kG, respectively. The dipolar term, $K_{s,dip}$ is rather small and anisotropic. The numbers for the spin terms in table 3 are based on the potential of Vosko *et al* (VWN) (1981). All three of those contributions depend on the choice of K_{xc}. However, due to the different signs of $K_{s,c}$ and K_{cp} the net effect on K is less significant than in the case of χ_{spin}. While, for example, the VWN potential yields $K_{s\parallel} = -0.0683\%$, for the total spin contribution, the largest values $K_{s\parallel} = -0.1588\%$ and -0.1324% result from the potentials JMW and GL, respectively. The main net contribution to K and also the significant anisotropy is due to $K_{orb,para}$ in accordance with the appreciable magnitude of χ^{val}_{orb}, especially its van Vleck part. From a Kramers–Kronig analysis investigating the importance of the individual bands for $K_{orb,para}$ we find that transitions between the occupied states and bands 4 to 7 causing the DOS peak around ϵ_F provide the main contributions. This is in line with the situation concerning χ_{orb}. It is also interesting to note, that terms off diagonal with respect to the two atoms in the HCP unit cell ($\kappa \neq \kappa'$ on the RHS of equations (2.6)) can be important. For $K_{orb,para}$ with $\boldsymbol{H} \perp c$, e.g. we obtain $K^{diag}_{orb,para} = 0.1837\%$, $K^{offdiag}_{orb,para} = 0.1589\%$.

Table 3. The Knight shift of Sc and its individual contributions in %.

	$K_{s,c}$	K_{cp}	$K_{s,dip}$	$K_{orb,para}$	$K_{orb,dia}$	K
$\boldsymbol{H}\parallel c$	0.179	−0.2193	−0.0280	0.2405	−0.0029	0.169
$\boldsymbol{H} \perp c$	0.179	−0.2193	0.0140	0.3426	−0.0029	0.314

To compare with experiments, we give $\langle K \rangle = \frac{1}{3}(K_\parallel + 2K_\perp) = 0.266\%$ and as a measure of the anisotropy, $K_{ax} = \frac{1}{3}(K_\parallel - K_\perp) = -0.048\%$. The corresponding experimental numbers (Carter *et al* 1977) are $\langle K \rangle = 0.29\%$ and $K_{ax} = -0.032\%$. These data, including the sign of the anisotropy, are in satisfactory agreement with our result.

According to table 4, where we display our calculated data for Ru, the situation is qualitatively similar to Sc. In the spin part the core polarization term tends to cancel the spin contact term, while $K_{s,dip}$ again gives rise to a small anisotropy in K. In spite of the large differences in the spin susceptibilities of Sc and Ru the numbers for $K_{s,c}$ are comparable, because the amplitudes of the radial s wavefunctions are much larger for Ru ($R_0^{2Ru}(0,\epsilon_F)/R_0^{2Sc}(0,\epsilon_F) = 5.42$). The s core shells 1 to 4 provide the following contributions to K_{cp}: −0.00676, −0.0364, −0.0069, and −0.0473% and the corresponding core hyperfine fields are -1×10^4, -5.4×10^4, -1.2×10^4, and -7.02×10^5 kG, respectively. $K_{orb,para}$ dominates also in Ru and is significantly larger than in Sc. This might be surprising at first sight if one considers the results for χ_{orb}. However, one should keep in mind that, in contrast to χ^{val}_{orb}, $K_{orb,para}$ probes the immediate vicinity of the nucleus and contains integrals of the form

$$I_d = \int \rho^2 d\rho \frac{1}{\rho^3} R_2^2(\rho, \epsilon_F). \tag{4.2}$$

Since the d wavefunction of the late-4d transition metal Ru is much more concentrated at smaller radii than that of the early-3d transition metal Sc, I_d^{Ru} can be expected to be significantly larger than I_d^{Sc}. In fact we obtain $I_d^{Ru}/I_d^{Sc} = 7.02$, a number

explaining the observed effect qualitatively. A Kramers–Kronig analysis demonstrates that similarly to Sc, bands in an extended energy region are important for both $K_{\mathrm{orb,para}}$ and $\chi^{\mathrm{val}}_{\mathrm{orb}}$. This is shown by figure 5 where we draw the spectral functions of the correlation functions determining $K_{\mathrm{orb,para}}$ (2.6) and the van Vleck part, $\chi^{\mathrm{val\,vV}}_{\mathrm{orb}}$, of (2.5). The peaks between 0.1 and 0.5 Ryd are the result of transitions between the occupied bands and bands 8 to 12.

Table 4. The Knight shift of Ru and its individual contributions in %.

	$K_{\mathrm{s,c}}$	K_{cp}	$K_{\mathrm{s,dip}}$	$K_{\mathrm{orb,para}}$	$K_{\mathrm{orb,dia}}$	K
$H\|\|c$	0.0945	−0.0973	−0.0122	0.5274	−0.0108	0.501
$H\perp c$	0.0945	−0.0973	0.0061	0.5470	−0.0108	0.539

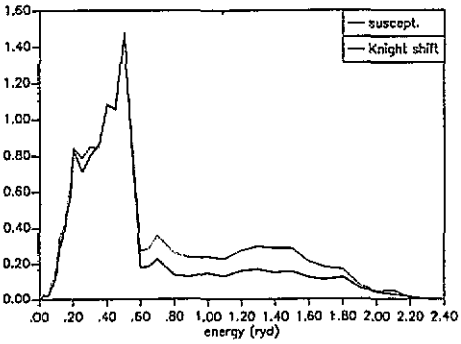

Figure 5. The spectral functions determining $\chi^{\mathrm{vV}}_{\mathrm{orb,para}}$ (——) and $K_{\mathrm{orb,para}}$ (·····) in arbitrary units.

The following experimental results have been most recently obtained by Burgstaller *et al* (1992): $K_{\|} = 0.56$ and $K_{\perp} = 0.46\%$. Whereas our value of 0.526% for $\langle K \rangle$ is reasonably near the measured one (amounting to 0.493%), there is a significant difference in the sign and the magnitude of the anisotropy.

Table 5. Nuclear moments, hyperfine fields and partial DOS for Sc^{45}, Ru^{99} and Ru^{101} in the notation of Asada and Terakura. μ_K and Q_K have been taken from Brevard and Granger (1981) for Ru and from Goldman (1972) for Sc.

	μ_K	Q_K		Hyperfine fields (10^6 Oe)			
Ru^{99}	−0.6381	0.076		H_{F}	$H^{\mathrm{p}}_{\mathrm{orb}}$	$H^{\mathrm{d}}_{\mathrm{orb}}$	H_{cp}
Ru^{101}	−0.7152	0.44	Ru	11.597	2.672	0.8646	−0.140
Sc^{45}	4.7562	−0.22	Sc	2.7974	0.6264	0.1238	−0.0564

	Partial DOS at ϵ_{F} (states/(spin Ryd atom dimension of representation))							
	$n^{\mathrm{s}}_{A_1'}$	$n^{\mathrm{p}}_{E'}$	$n^{\mathrm{p}}_{A_1''}$	$n^{\mathrm{d}}_{E''}$	$n^{\mathrm{d}}_{E'}$	$n^{\mathrm{d}}_{A_1'}$	$\|\Omega^{\mathrm{sd}}_{A_1'}\|$	$\|\Omega^{\mathrm{pd}}_{E'}\|$
Ru	0.071	0.136	0.120	0.998	1.153	0.951	0.0295	0.0129
Sc	0.248	1.389	1.041	1.065	2.552	3.454	0.138	1.175

Table 6. The spin–lattice relaxation times of Sc^{45}, Ru^{99}, and Ru^{101} together with their individual contributions. $1/(T_1T)$ is in $s^{-1}K^{-1}$.

		Orbital		Dipole		Quadrupole		Core
	Contact s	p	d	p	d	p	d	polarization
Sc^{45} ($H\|\|c$)	0.7877×10^{-1}	0.1851	0.8239×10^{-1}	0.6636×10^{-1}	0.8751×10^{-2}	0.4567×10^{-3}	0.5782×10^{-4}	0.1413×10^{-1}
Sc^{45} ($H \perp c$)	0.7877×10^{-1}	0.2160	0.1092	0.6033×10^{-1}	0.8510×10^{-2}	0.3784×10^{-3}	0.7509×10^{-4}	0.1413×10^{-1}
Ru^{99} ($H\|\|c$)	0.3872×10^{-2}	0.1337×10^{-2}	0.4430×10^{-1}	0.4322×10^{-3}	0.3333×10^{-2}	0.2294×10^{-4}	0.1693×10^{-3}	0.6278×10^{-3}
Ru^{99} ($H \perp c$)	0.3872×10^{-2}	0.1427×10^{-2}	0.4931×10^{-1}	0.4139×10^{-3}	0.3414×10^{-2}	0.2105×10^{-4}	0.1856×10^{-3}	0.6278×10^{-3}
Ru^{101} ($H\|\|c$)	0.4864×10^{-2}	0.1680×10^{-2}	0.5566×10^{-1}	0.5430×10^{-3}	0.4187×10^{-2}	0.7689×10^{-3}	0.5674×10^{-2}	0.7887×10^{-3}
Ru^{101} ($H \perp c$)	0.4864×10^{-2}	0.1793×10^{-2}	0.6195×10^{-1}	0.5200×10^{-3}	0.4289×10^{-2}	0.7056×10^{-3}	0.6222×10^{-2}	0.7887×10^{-3}

	p–d orbital	p–d dipole	p–d quadrupole	s-contact core polarization	s-contact d dipole	p-dipole core polarization	d-orbital core polarization	$1/(T_1T)$ total
Sc^{45} ($H\|\|c$)	0.0	-0.9975×10^{-3}	0.0	-0.9848×10^{-3}	-0.3088×10^{-3}	-0.3181×10^{-2}	0.6871×10^{-5}	0.4306
Sc^{45} ($H \perp c$)	-0.3491×10^{-1}	-0.2494×10^{-2}	0.2589×10^{-4}	-0.9848×10^{-3}	0.1544×10^{-3}	0.1591×10^{-2}	-0.3436×10^{-5}	0.4508
Ru^{99} ($H\|\|c$)	0.0	-0.1264×10^{-6}	0.0	-0.1627×10^{-4}	-0.1434×10^{-4}	-0.1434×10^{-6}	-0.7554×10^{-4}	0.5399×10^{-1}
Ru^{99} ($H \perp c$)	-0.4423×10^{-5}	-0.3160×10^{-6}	0.3180×10^{-7}	-0.1627×10^{-4}	0.7169×10^{-5}	0.7169×10^{-7}	0.3777×10^{-4}	0.5930×10^{-1}
Ru^{101} ($H\|\|c$)	0.0	-0.1588×10^{-6}	0.0	-0.2043×10^{-4}	-0.1801×10^{-4}	-0.1801×10^{-6}	-0.9490×10^{-4}	0.7403×10^{-1}
Ru^{101} ($H \perp c$)	-0.5557×10^{-5}	-0.3969×10^{-6}	0.1066×10^{-5}	-0.2043×10^{-4}	0.9006×10^{-5}	0.9006×10^{-7}	0.4745×10^{-4}	0.8116×10^{-1}

Table 7. Interacting ($B_{s,c}$) and non-interacting ($B^{P}_{s,c}$) integrand for the spin contact term of $(1/T_1T)$. The q-dependent static spin susceptibilities and the Stoner enhancements are tabulated for comparison. The B are measured in atomic units, the susceptibilities are in units of 10^{-6} emu mol^{-1} and q is in units of $2\pi/a$; $q_y = 0$. We employ the K_{xc}, resulting from the VWN potential.

q vector							
q_x	q_z	$B_{s,c}$	$B^{P}_{s,c}$	$B_{s,c}/B^{P}_{s,c}$	$\chi^{s}(q,q;0)$	$\chi^{Ps}(q,q;0)$	$S(q)$
0	0.15	4307.8	195.03	22.088	465.5	68.92	6.76
0	q_z^{BZ}	7193.0	208.35	34.52	339.5	70.90	4.79
0.05	0	8821.6	1915.1	4.606	185.1	64.50	2.87
0.05	0.15	2738.2	181.63	15.076	442.8	72.67	6.093
0.05	q_z^{BZ}	3148.9	45.74	68.844	441.1	70.09	6.34
0.25	0	1502.9	382.02	3.934	137.2	54.07	2.54
0.25	0.15	680.17	172.06	3.953	184.1	58.19	3.16
0.25	q_z^{BZ}	1083.1	61.94	17.487	223.9	60.91	3.68
0.5	0	467.47	214.63	2.178	82.28	43.66	1.89
0.5	0.15	220.92	111.84	1.975	92.33	44.45	2.08
0.5	q_z^{BZ}	105.82	39.83	2.657	41.15	24.20	1.70
2/3	0	625.81	277.72	2.253	60.26	35.13	1.72

4.3. The spin–lattice relaxation

Whereas experimental measurements of $1/T_1$ for Sc, obtained at room temperature, date back to the 1960s (Masuda and Hashimoto 1969, Ross *et al* 1969, Narath and Fromhold Jr 1967), measurements for Ru have been undertaken only very recently (Burgstaller 1992). $1/T_1$ for Sc has been calculated by Asada and Terakura (1982) using their LMTO–ASA band-structure results. We performed calculations based on our KKR bandstructure for both substances and $\boldsymbol{H}$ parallel and perpendicular to the c axis. In the case of Ru we considered the two isotopes Ru^{99} and Ru^{101}. A detailed account of the results, neglecting many-body effects, is given by table 6, where we use exactly the same symbols that are explained in the paper of Asada and Terakura. However, in contradistinction to them we apply the scalar relativistic expressions of Blügel *et al* (1987). In table 5 we gather the nuclear and the electronic quantities determining $1/T_1$ in this approximation, namely, the nuclear magnetic dipole- (μ_K) and quadrupole- (Q_K) moments on the one hand and the symmetry-adapted partial DOS at ϵ_F, including the finite angular momentum off-diagonal matrix elements, $\Omega^{Sd}_{A_1'}$ and $\Omega^{pd}_{E'}$, of the imaginary part of the one-particle Green's function and the hyperfine fields on the other. Terms up to $l_{max} = 2$ have been taken into account. The order-of-magnitude difference between the data for Ru and Sc is due to the fact that the influence of the larger hyperfine fields of Ru is overcompensated by the differences of μ_K and of the partial DOS components in favour of Sc. In both substances all the terms non-diagonal in the angular momentum components and/or the interactions (second half of table 6) turn out to be fairly unimportant. Rather striking, in the case of Sc, is the big share of the p orbital term which is due to a relatively high p DOS at ϵ_F. The differences in the values of the two Ru isotopes is an immediate consequence of the variance in their μ_K. Since in metals the terms depending on Q_K are generally much smaller than those containing μ_K the huge difference of the nuclear quadrupole moment between the two Ru isotopes influences T_1 only moderately. Nevertheless the d quadrupole contribution of Ru^{101} is substantial. For both substances $1/T_1$ is slightly larger for $\boldsymbol{H} \perp c$ than for $\boldsymbol{H} \| c$ opposite to the Knight shifts. Though the

results are based on different bandstructure methods, our hyperfine fields and partial DOS for Sc are comparable to those of Asada and Terakura. The main difference lies in the off-diagonal quantity $\Omega^{pd}_{E'}$, which is substantially smaller in our case. Our core polarization contributions are smaller, since we treat the core electrons within the SDFA instead of the unrestricted Hartree–Fock approximation. The net numbers for $1/T_1$, however, are in close agreement. For Sc the experimental room-temperature data for $\langle 1/T_1T\rangle$ obtained by Masuda and Hashimoto (1969), Ross *et al* (1969), and Narath and Fromhold Jr (1967) are 0.68 ± 0.09, 0.92 ± 0.08, and 0.63 ± 0.04 $s^{-1}K^{-1}$, respectively. To investigate the cause of this difference between the experimental and the theoretical values we considered many-body enhancement effects in the spin terms of $1/T_1$ for Sc within the SDFA–RPA. To start with the spin contact term, equations (2.8) and (2.11) yield

$$\left(\frac{1}{T_1T}\right)_{s,c} = \frac{4\pi k_B}{\hbar}\left(\tfrac{2}{3}\hbar\gamma_N\mu_B\right)^2 2\sum_{\substack{\nu_1\nu_2\\ \nu_3\nu_4}} R_{0\nu_1}(0)R_{0\nu_2}(0)R_{0\nu_3}(0)R_{0\nu_4}(0)\lim_{\omega_0\to 0}$$
$$\times\int\frac{dq}{\Omega_{BZ}}\frac{1}{\omega_0}\,\mathrm{Im}\,\hat{\chi}^{S\kappa\kappa}_q(0000\nu_1\nu_2,0000\nu_3\nu_4;\omega_0)$$
$$=\frac{4\pi k_B}{\hbar}\left(\tfrac{2}{3}\hbar\gamma_N\mu_B\right)^2 2\int\frac{dq}{\Omega_{BZ}}B_{s,c}(q). \tag{4.3}$$

Here, the indices ν_i (running from 1 to 3 in the present application) take care of the energy dependence of the radial wavefunctions R which is important when calculating the enhanced quantities at fine q. Replacing $B_{s,c}$ with the corresponding non-interacting quantity, $B^P_{s,c}$, we end up with the usual formula for $(\frac{1}{T_1T})_{s,c}$ in terms of the s DOS at ϵ_F and the number given in table 6. Equation (4.3) again refers to the non-relativistic case and may easily be cast into the scalar relativistic form by replacing the radial functions by the integrals as derived by Blügel *et al* (1987). We have evaluated the wavevector- and frequency-dependent spin susceptibility of scandium for a number of q-points in the IWBZ and collect the results, relevant for the present problem, in table 7. We compare the quantities $B_{s,c}$, $B^P_{s,c}$, and their ratios on the one hand to the static interacting and non-interacting susceptibilities and the Stoner enhancement factors on the other hand. There is no general q-independent relation between some power of $S(q)$ and the interaction effects on the spin contact term. In some parts of the phase space, especially for q in the (1,0,0) direction, they scale with a power greater than the square of $S(q)$, whereas in other parts they behave rather moderately. In the regions with the largest enhancement effects, the phase-space weighted $B^P_{s,c}$ is relatively small, while for larger values of q_x, q_y the influence of the enhancement is reduced to factors near 2 with increasing tendency towards the BZ boundary. In view of the observed, rather strong q-dependence of the relevant quantities an exact evaluation of $T_{1s,c}$ would require one to determine $\hat{\chi}_q(\rho,\rho',\omega)$ on a rather dense mesh within the BZ, an extremely tedious task. However, the data collected in table 7 allow one to determine $T_{1s,c}$ to a reasonable approximation. For this purpose we write the BZ integral of equation (4.3) in the following form

$$I^{(P)}(q) = n_{IWBZ}\int_0^{\pi/6}d\phi\int_0^{q_z^{BZ}}dq_z\int_0^{q^{BZ}(\phi)}dq_\rho q_\rho F^{(P)}(\phi)$$
$$F^{(P)}(\phi) = \int_0^{q_z^{BZ}}dq_z\int_0^{q^{BZ}(\phi)}dq_\rho q_\rho B^{(P)}_{s,c}(q)\Big/\int_0^{q_z^{BZ}}dq_z\int_0^{q^{BZ}(\phi)}dq_\rho q_\rho. \tag{4.4}$$

Here, $n_{\mathrm{IWBZ}} = 24$, is the number of the IWBZ and the integrals go over one prismatic IWBZ. The data collected in table 7 allow for interpolating $B^{(\mathrm{P})}_{\mathrm{s,c}}$ within the q_x–q_z plane and subsequently evaluating $F^{(\mathrm{P})}(0)$. Assuming angular isotropy of $\mathrm{F}^{(\mathrm{P})}(\phi)$ we conclude that enhancement effects increase $T^{-1}_{1\mathrm{s,c}}$ by a factor of about 3.3, leading to $(T_1T)^{-1}_{\mathrm{s,c}} \simeq 0.236\ \mathrm{s^{-1}K^{-1}}$ instead of the number 0.0788 quoted in table 7. We found that interaction effects on the spin dipolar terms are less dramatic and give rise to an increase in these contributions by a factor of about 1.5. Altogether we end up with $(T_1T)^{-1} \simeq 0.63\ \mathrm{s^{-1}K^{-1}}$, a number in the range of the experimental data. It is gratifying to remark that the evaluation of the spin contact term using the non-interacting susceptibility at the same q points as the enhanced susceptibility and applying the isotropy assumption leads to almost the same value for $(T_1T)^{-1}_{\mathrm{s,c}}$ as obtained with the formula containing the s DOS at ϵ_{F}, the deviation amounting to less than 10%.

For Ru we did not include interaction effects. Since the long-wavelength Stoner enhancement factor of this substance is low, we expect them to be rather insignificant. The measurements of Burgstaller (1992) for Ru, performed at He temperatures, yield $(T_1T)^{-1} = 0.063$ and $0.077\ \mathrm{s^{-1}K^{-1}}$ in the case of $\mathrm{Ru^{99}}$ and $\mathrm{Ru^{101}}$, respectively. The agreement with our theoretical data is good. We have just learned of the most recent calculations of $(T_1T)^{-1}$ for Ru by Markendorfer (1992), whose numbers, emerging from a fully relativistic treatment are very close to ours.

5. Summary

We gave a quantitative account of the low-temperature susceptibilities and the nuclear resonance behaviour of the HCP d transiton metals Sc and Ru on the basis of magnetic correlation functions. In this unified approach it became apparent that these quantities depend sensitively and differently on the details of the electronic structure of the substance in question. Not only the Fermi surface properties but the bandstructure in a finite energy range, which were explored by the present method, are important. The behaviour of the correlation functions in different regions of the real and the reciprocal space is probed and a quantitative treatment of all those quantities was only possible because—within the SDFA–RPA—we were able to evaluate these functions in full dependence on their arguments. Whereas static and long-wavelength correlations go into the homogeneous susceptibilities and the Knight shifts, for spin–lattice relaxation the whole BZ has to be considered, once interaction effects are taken into account. In the case of Sc we have shown that this becomes a true low-frequency dynamical problem since these effects cannot be adequately expressed by static quantities like the q-dependent Stoner factors squared as suggested by theories based on the homogeneous electron gas model. We have also demonstrated that the rapidly varying behaviour at finite wavevectors cannot be derived from the features at small q and that the correlation functions are not interconnected by simple relations. In view of the approximations, unavoidable in a many-body problem of this kind, the results of our SDFA–RPA approach are reasonably near to the experimental data and describe the trends correctly.

Acknowledgments

We are grateful to H Ebert and A Burgstaller for drawing our attention to the scalar relativistic formulae and communicating their experimental data to us.

References

Asada T and Terakura K 1982 *J. Phys. F: Met. Phys.* **12** 1387

Benkowitsch J and Winter H 1983 *J. Phys. F: Met. Phys.* **13** 991

Bertani R, Mali M, Roos J and Brinkmann D 1990 *J. Phys.: Condens. Matter* **2** 7911

Bloembergen N and Rowland T J 1953 *Acta Metall.* **1** 731 (erratum 1955 *Acta Metall.* **3** 74)

Blügel S, Akai H, Zeller R and Dederichs P H 1987 *Phys. Rev.* B **35** 3271

Brevard C and Granger P 1981 *J. Chem. Phys.* **75** 4175

Burgstaller A 1992 Private communication

Burgstaller A, Ebert H and Voitländer J 1992 *Proc. IXth Int. Conf. on Hyperfine Interactions (Toyonaka, Japan, 1992)*

Carter G C, Bennett L H and Kahan D J 1977 Metallic Shifts in NMR Part 1 *Prog. Mater. Sci.* **20** (Oxford: Pergamon) pp 321–4

Das S G 1976 *Phys. Rev.* B **13** 3978

Ebert H and Akai H 1992 *Preprint*

Goldman D T 1972 *American Institute of Physics Handbook* 3rd edn (New York: McGraw-Hill) table 8b-1

Götz W and Winter H 1991 *J. Phys.: Condens. Matter* **3** 8931

—— 1992a *J. Phys.: Condens. Matter* **4** 6253

—— 1992b *Solid State Commun.* **82** 457

Gunnarsson O and Lundqvist B I 1976 *Phys. Rev.* B **13** 4274

Guthrie A N and Bourland L T 1931 *Phys. Rev.* **37** 303

Isaacs L L and Lam D J 1970 *J. Phys. Chem. Solids* **31** 2581

Jaccarino V 1967 *Proc. Int. School of Physics Enrico Fermi Course XXXVII* (New York: Academic) pp 335–85

Janak J, Moruzzi V L and Williams A R 1975 *Phys. Rev.* B **12** 1257

Jepsen O, Andersen O K and Mackintosh A R 1975 *Phys. Rev.* B **12** 3084

Kojima H, Tebble R S and Williams D E G 1961 *Proc. R. Soc.* A **260** 237

MacDonald A H and Vosko S H 1979 *J. Phys. C: Solid State Phys.* **12** 2977

Markendorfer R 1992 Private communication

Masuda Y and Hashimoto M 1969 *J. Phys. Soc. Japan* **26** 1058

Matsumoto M, Staunton J B and Strange P 1991 *J. Phys.: Condens. Matter* **3** 1453

Moriya T 1963 *J. Phys. Soc. Japan* **18** 516

Narath A 1967 *Hyperfine Interactions* (New York: Pergamon) pp 283–363

Narath A and Fromhold Jr T 1967 *Phys. Lett.* **25A** 49

Perdew J P and Zunger A 1981 *Phys. Rev.* B **23** 5048

Rajagopal A K 1980 *Adv. Chem. Phys.* **XLI** 59

Ross J W, Fradin F Y, Isaacs L L and Lam D J 1969 *Phys. Rev.* **183** 645

Spedding F H and Croat J J 1973 *J. Chem. Phys.* **58** 5514

Stenzel E and Winter H 1985 *J. Phys. F: Met. Phys.* **15** 1571

—— 1986 *J. Phys. F: Met. Phys.* **16** 1789

Stierman R J, Gschneidner K A Jr, Tsang T W E, Schmidt F A, Klavins P, Shelton R N, Queen J and Legvold S 1983 *J. Magn. Magn. Mater.* **36** 249

von Barth U and Hedin L 1972 *J. Phys. C: Solid State Phys.* **5** 1629

Vosko S H and Perdew J P 1975 *Can. J. Phys.* **53** 1385

Vosko S H, Wilk L and Nusair M 1980 *Can. J. Phys.* **58** 1200

Winter H, Szotek Z and Temmerman W M 1992 *Applications of Multiple Scattering Theory to Materials Science* (Materials Research Society Pittsburg, PA) pp 71–83